Appendix 2

Submitted to: The 7th International Biennial Conference on Physics of Estuaries and Coastal Seas

THE ROLE OF THERMAL STRATIFICATION IN TIDAL EXCHANGE AT THE MOUTH OF SAN DIEGO BAY

D.B. Chadwick

Environmental Sciences Division
Naval Command, Control &
Ocean Surveillance Center
San Diego, CA

J.L. Largier

Center for Coastal Studies
Scripps Institution of Oceanography
La Jolla, CA

and

R.T. Cheng

Water Resource Division
U. S. Geological Survey
Menlo Park, CA 94025

Abstract

We have examined, from an observational viewpoint, the role of thermal stratification in the tidal exchange process at the mouth of San Diego Bay. In this region, we found that both horizontal and vertical exchange processes appear to be active. The vertical exchange in this case is apparently due to the temperature difference between the bay water and ocean water. We found that the structure of the outflow, and the nature of the tidal exchange process both appear to be influenced by thermal stratification. The tidal outflow is found to lift-off from the bottom during the initial and later stages of the ebb flow when barotropic forcing is weak. During the peak ebb flow, the mouth section is flooded, and the outflow extends to the bottom. As the ebb

flow weakens, a period of two-way exchange occurs, with the surface layer flowing seaward, and the deep layer flowing into the bay. The structure of the tidal-residual flow and the residual transport of a measured tracer are strongly influenced by this vertical exchange. Exchange appears to occur laterally as well, in a manner consistent with the tidal-pumping mechanism. Tidal cycle variations in shear and stratification are characterized by strong vertical shear and breakdown of stratification during the ebb, and weak vertical shear and build-up of stratification on the flood. Evaluation of multiple tidal-cycles from time-series records of flow and temperature indicate that the vertical variations of the flow and stratification observed during the cross-sectional measurements are a general phenomenon during the summer. Together, these observations suggest that thermal stratification can play an important role in regulating the tidal exchange of low-inflow estuaries.

Introduction

We have recently examined some aspects of the tidal exchange process at the mouth of San Diego Bay, CA. The horizontal and vertical structure of the exchange were studied to gain insight into the predominant mechanisms controlling the export of water-borne contaminants out of the bay. Petroleum hydrocarbons from chronic sources within the bay present a significant environmental concern, and also provide a useful tracer for distinguishing bay water from oceanic water. Previous studies of the tidal exchange process have focused on two general mechanisms. In a coastal embayment, with negligible freshwater inflow, horizontal asymmetries between the ebb and flood tides lead to net tidal exchange through the tidal pumping mechanism (Stommel and Farmer, 1953, Signell and Butman, 1992). In estuaries with significant freshwater inflow, vertical density driven exchange is significant and may dominate the net tidal exchange

(Dyer, 1974).

At the mouth of San Diego Bay, we found that both horizontal and vertical exchange processes appear to be active. This is somewhat surprising in view of the absence of freshwater inflow to the bay during most of the year. The vertical exchange in this case is apparently due to the temperature difference between the bay water and ocean water. The resulting temperature-dominated density gradient leads to two related effects which influence the bay-ocean exchange including, (1) a period of stratified exchange between the outer bay and the ocean, primarily during the ebb-flood transition, and (2) the lift-off of the ebb flow as it exits the mouth of the bay. The first effect can be expected to enhance the tidal exchange directly, while the lift-off may lead to structural variations in the outflow which indirectly effect the exchange due to tidal pumping.

In this paper, we set out to provide a description of this tidal exchange process at the mouth of San Diego Bay, and investigate the role of thermal stratification in modifying the exchange. The first section describes the limited existing knowledge of the circulation and hydrography of San Diego Bay, followed by a description of the field effort undertaken for this study. From the field observations, we develop a descriptive view of the summer conditions within the bay as a whole, and in the mouth region in particular. The lift-off of the ebb flow and the subsequent vertical-exchange during the reversal to flood are resolved and evaluated on the basis of the outflow Froude number. A qualitative comparison of vertical and horizonal exchange is made on the basis of the residual transport at the mouth section, and a temperature-tracer mixing diagram. The generality of the observed vertical structure is evaluated in terms of tidal cycles of vertical velocity-shear and stratification from moored time-series measurements of velocity and temperature near the mouth. A mechanistic description of the development of these

"thermal estuary" characteristics and comparison to other low-inflow estuaries is provided in a companion paper (Largier, et al., 1995a).

Description of the Study Site

San Diego Bay is relatively long and narrow, 25 km in length and 1-3 km wide, forming a crescent shape between the City of San Diego on the north, and Coronado Island/Silver Strand on the south (Figure 1). Exchange with the ocean is limited to a single channel at the mouth. This north-south channel is about 1.2 km wide, bounded by Point Loma on the west and Zuniga jetty on the east, with depths between 5-15 m. The bay hydrograph is characterized by small annual freshwater inflow (mean rainfall ≈ 26 cm year^{-1}), with zero inflow during most summers. The currents within the bay are dominated by a mixed diurnal-semidiurnal tidal forcing, with a dominant semidiurnal component (Peeling, 1974). The tidal range from MLLW to MHHW is about 1.7 m with extreme tidal amplitudes close to 3 m. Recent bottom mounted ADCP measurements at the mouth indicate current velocities ranging from 0.2-0.8 m s^{-1} (Cheng and Gartner, 1993). Near the mouth, historical observations (Hammond, 1976, Navy, 1950, Smith, 1970), and the ADCP data suggest a net inflow at the bottom, with the bottom flood-tide velocities leading the surface velocities by about 30 to 90 minutes. Hammond (1976) attributed this inflow to a net northward bottom transport in the ambient flow outside the bay, based on seabed drifter trajectories. However, the ADCP records indicate net landward flow near the bottom is enhanced during periods of neap tide, suggesting that baroclinic circulation may be significant during these episodes.

Surface and bottom water temperatures in San Diego Bay exhibit a seasonal cycle with an amplitude of about 8-9 °C (Smith, 1972). During the summer period net heat flux to the bay and

limited exchange with the ocean lead to the development of both vertical and longitudinal temperature/density gradients in the bay. Smith (1972) found maximum vertical temperature gradients of about 0.5 °C m^{-1} during the summer. Typical longitudinal temperature gradients of about 7-10 °C over the length (~0.3-0.5 °C km^{-1}) of the bay have been reported (Federal Water Pollution Control Administration, 1973, Largier et al., 1995b) during the summer months. Spectral analysis of a year-long time series of surface and bottom temperature showed significant peaks at the diurnal and semidiurnal tidal periods, as well as at periods of 8.2, 5.1, and 4.2 (surface only) hours (Smith, 1972). The 8.2 hour response was explained as an interaction between the diurnal and semidiurnal tidal constituents, while the 5.1 and 4.2 hour periods were attributed to a possible seiche.

Field Measurements

A series of observations were undertaken during 1993-94 to examine the dynamics which regulate the exchange of bay water with ocean water in the region of the mouth. The observations included bottom-moored ADCP and thermistor records, ADCP/CTD surveys across the mouth of the bay and in the region of the outflowing jet, and axial CTD surveys of the entire bay. In conjunction with the CTD measurements, a flow-through fluorometer was used to measure hydrocarbon concentrations using an ultra-violet fluorometric (UVF) technique as described by Katz and Chadwick (1991).

During the period June 22 to July 23, 1993, a broadband 1.2 MHz ADCP was deployed upward-looking at a bottom depth of about 15 meters just inside the mouth. Data were recorded continuously at a 10-minute interval, providing a temporal record of the vertical flow structure at resolution of 1 meter. Self-recording thermistors were deployed at buoy stations along the axis

of the bay at 9 locations, and temperature were recorded every 9.6 minutes during the period 29 July to 22 August, 1993. A transect across the mouth of the bay was repeated 31 times through a ~12 hour, semidiurnal, symmetrical tidal cycle on 18 May, 1994. A 1.2 MHz narrow-band shipboard ADCP and towed CTD/UVF were used to measure water properties and flow at the section. The CTD/UVF system was profiled while underway to obtain a continuous series of 12 profiles across the mouth. A series of nine surveys of the region outside the mouth were performed the following day (19 May, 1994), during tidal conditions similar those of the cross-mouth transects. The surveys consisted of a series of transverse and axial transects in the region extending from ~1 km inside the mouth to ~5 km offshore from the mouth. Current meters and thermistors were deployed on sub-surface moorings at three locations off the mouth during the period 17-19 May, 1994. A series of CTD/UVF vertical profiles were obtained along the axis of the entire bay on 17 May, 1994. Transect lines and mooring locations are shown in Figure 1.

Results & Discussion

San Diego Bay Axial-Sections

Typical summer conditions for the axial temperature, salinity, density, and UVF tracer distributions in San Diego Bay were developed from the vertical profiles of 17 May, 1994 (Figure 2a). The plots show several interesting points. The density field is dominated by the effects of temperature except at the head of the bay where hypersaline conditions have begun to develop (see also Largier et al., 1995a). The overall longitudinal temperature difference in the bay is about 4-5 °C, with a local gradient near the mouth of about 0.5 °C km^{-1}. The

temperature/density field progresses from well mixed in the inner bay, to a partially mixed condition in the outer bay where the proximity of the cooler ocean water is evident in the enhanced vertical stratification. The vertical gradient in the mid to inner bay is generally less than 0.05 °C m^{-1}, while near the mouth, the gradient increases to about 0.3 °C m^{-1}. The UVF distribution clearly indicates the primary source of hydrocarbons in the inner bay, and also illustrates the influence of stratification in the outer bay on the tracer distribution. The hydrocarbon influx is considered to be relatively steady, resulting from the leaching of polycyclic aromatic hydrocarbons from creosote impregnated pier pilings (Katz et al, in prep.). Unstratified winter conditions from a similar axial transect on 14 January, 1994 are shown in Figure 2b for comparison. The thermal structure is absent in winter, while the hypersalinity still persists resulting in a weak inverse density gradient. This period is typically followed by rain events which lead to sub-ocean salinities in the inner bay.

Outflow Mapping

Surface water conditions off the mouth were examined with a series of near-synoptic maps developed from the surveys of 19 May, 1994 (see Figure 1). The tracer (Figure 3) and velocity fields indicate that the outflow which starts as a radial structure from the mouth, develops into a low-aspect jet-like structure with a streamwise scale of about 5 km. When the flow reverses to flood, the outflow water is "pinched off" laterally at the mouth, and then drifts to the east under the influence of the longshore currents while continuing to disperse. This view of the horizontal exchange is conceptually consistent with the tidal pumping model suggested by Stommel and Farmer (1952), but it is significantly distorted by the longshore flow and the topographical complexity of the study area.

Mouth Sections

An alternate view of the exchange process, and especially of the potential thermal-buoyancy effects, is obtained from the transverse and axial sections performed near the mouth where the stratification is strongest. A tidal sequence of the transverse sections for velocity, temperature, and UVF was developed from a subset of the cross-sectional transects from the 18 May, 1994 survey (Figure 4a-c). The sequence begins at the slack flood and progresses through the ebb/flood cycle to the subsequent slack flood. We find that the ebb-flow velocities are significantly stronger at the surface with vertical shear $\Delta U_z = O(0.2\ m\ s^{-1})$ during much of the ebb period. The transition from ebb to flood is characterized by a period of vertical exchange flow lasting about 2 hours during which the surface water continues to ebb while the bottom water has reversed to flood. The flood tide velocities are significantly more uniform in the vertical, and the flood-ebb transition of the surface and bottom velocities occurs approximately in phase. From the temperature profiles, we find the thermocline at a high-water depth of about 6 meters. The vertical temperature difference is about 3 °C, leading to a density difference of about 0.5 kg/m^3. The pronounced thermocline present at slack high-water breaks down during the ebb flow and then rebuilds during the subsequent flood. During the flood tide, the thermocline also displays a significant cross-stream slope, presumably due to the influence of a relatively strong (10-15 knot) westerly wind during the afternoon. The UVF sections show the bay water concentrated in the surface layer during the ebb, the appearance of ocean water initially at the channel sides associated with the "pumping" process, and the subsequent return-flow of mixed bay/ocean water at mid-depth.

The axial sections through the mouth region show quite clearly the thermal structure that drives the observed variations in velocity and stratification at the mouth (Figures 4-5). At slack

high water, a cold thermal-wedge can be seen extending into the bay, enhancing the vertical density gradient near the mouth. In the early ebb, the velocity is weak and the outflow lifts off as it encounters the thermal wedge. As the ebb flow develops in strength, the thermal wedge is broken down by the strong vertical shear, and advected seaward, the southward velocity extending to the bottom. As the ebb weakens, the flow again seperates from the bottom, developing into a vertical exchange flow during the transition from ebb to flood. As the flood tide builds, the cold thermal wedge rebuilds and intrudes into the bay with a steep frontal feature reminiscent of a density current.

Buoyancy Effects

The temporal variation in velocity and density is extracted from the sectional data by looking at sectional properties (u,ϱ) above and below the average level of the pycnocline at about 6 meters. Plotting this confirms that the bottom velocities are significantly lower than the surface velocities during the ebb flow, while the velocity difference during the flood becomes negligible as the tide approaches peak flow (Figure 7). We find also that the bottom flow reverses approximately 1-2 hours (depending on the depth) ahead of the surface flow during the ebb-flood transition, resulting in a significant period of exchange flow during which the surface and bottom flow are of opposite sign. The internal hydraulic balance of the thermal-driven buoyancy forces and the barotropic tidal forcing for each layer is characterized by the Froude number (Armi and Farmer, 1986) as

$$F_i = \frac{U_i}{\sqrt{g' h_i}}$$

where U_i is the layer velocity, g' is the reduced gravity, and h_i is the layer depth. Neglecting frictional effects and mixing, Armi and Farmer showed that strong tidal-forcing of a simple two-layer exchange flow through a topographic expansion leads to a progression of flow conditions. Beginning with a two-layer, baroclinic exchange-flow during the slack tide, the flow structure progresses to an arrested-wedge condition as the barotropic forcing increases, and finally to a fully-flooded condition in which one layer fills the entire section. In this progression, the transition from two-layer exchange-flow, to the arrested conditions occurs when $F_i \approx 1$.

For the San Diego Bay mouth region, the topographic expansion is replaced by the hydrodynamic expansion of the outflowing tidal-jet. For purposes of a simple analysis, the surface and bottom layers were defined by the zero velocity interface height in the main-channel region from the cross-sectional measurements at the mouth. Examining the progression of the Froude number and velocity based on the observations, we find qualitative agreement with this model during the ebb-flood transition, with periods of supercritical flow corresponding to strong barotropic forcing and subcritical flow during the slack water (Figure 7). The weak vertical exchange during the flood-ebb transition (see Figure 4a) might be explained by the effects of bottom friction in damping the velocity of the lower "layer" during the flood tide. This damping is apparent in the axial velocity sections through the mouth (Figure 6).

Tidal Exchange

To evaluate the effect of thermal stratification on tidal exchange, tidal residual sections

were constructed for axial velocity, UVF concentration, and UVF transport, based on the 31 cross sectional transects on 18 May, 1994 (Figure 8). From this analysis, we find that the residual velocity displays a significant vertical structure, with a tidally averaged surface outflow of O(5 cm/s) and bottom inflow of O(0.1 m s^{-1}). Lateral variations in the residual flow field are also present with enhanced outflow on the eastern portion of the channel. This is inconsistent with coriolis effects and could be attributed to upstream topography, wind-driven lateral circulation, or cross-channel variations in depth. The tidal residual UVF section also shows significant vertical variation with highest concentrations near the surface O(15 μg l^{-1}) and lower concentrations at depth O(10 μg l^{-1}). From the resulting net tidal transport of UVF we find that the residual field is characterized by an clear vertical-exchange structure.

A qualitative comparison of vertical and horizonal exchange can be made on the basis of a Temperature-UVF mixing diagram. For this purpose, we identify three primary water masses, the bay water which is warm and high UVF, the surface ocean water which is warm and low UVF, and the sub-thermocline ocean water which is cold and low UVF (Figure 9). The mixing line described by sectional averages from the mouth transects follows a distinctive cycle through the tide. Starting at slack high water, we find cold, low UVF water associated with the intrusion of ocean water into the mouth region. As the ebb flow develops, temperature and UVF both increase due to the influence of outflowing bay water. At the slack low water, the temperature and UVF reach a maximum. On the reversal to flood, we find that initially the UVF levels drop dramatically while the temperature remains high. This is indicative of the lateral exchange of surface ocean water and bay water associated with the tidal pumping process described by the horizontal mapping surveys. At a point approximately midway through the flood tide, the temperature drops rapidly, indicating the vertical intrusion of the sub-thermocline, oceanic water

associated with the vertical exchange. This cold water intrusion carries with it slightly elevated UVF levels, possibly associated with vertical mixing during the outflow. It is important to recognize that the mixing diagram is not necessarily indicative of true mixing, since the points are derived from sectional averages, but describes mixing in the sense of bulk tidal exchange of waters between the bay and ocean.

Generalization to a Longer Time-Series

To examine the generality of this process, we evaluated the one-month time series from the bottom mounted ADCP, and the vertical thermal structure from a five day period of similar tides (Figures 10-11). We find that the vertical structure and response to thermal buoyancy and tidal barotropic forcing of the flow at this station near the mouth is similar to that suggested by the transverse sections at the mouth. Strong vertical shear observed consistently during ebb tides (0.1-0.3 m s^{-1}) is generally absent during the floods. Reversal of the bottom currents during the ebb-flood transition tends to occur before the surface reversal, especially during neap tide periods. In addition, vertical shear during the neaps is comparable to or greater than during the springs, suggesting enhanced baroclinic circulation during periods of weak tidal mixing.

The tidal variation of surface-bottom temperature difference during the 5 day period 29 July - 2 August, 1994 (Julian date 211-215) indicates that the stratification often builds and peaks during the transition from ebb to flood flow. Flood tide periods gnerally exhibit stratitified conditions. On strong ebb-flows, the thermal stratification may break down entirely, while on weaker ebbs, only a partial breakdown may occur. This is generally consistent with the cross sectional observations during a moderate ebb flow during which a partial breakdown of the stratification was observed (Figure 7). This cycle of stratification is in contrast to the recent

results of Nunes-Vaz and Simpson (1994) where the effect of straining of the longitudinal density gradient by the vertical shear (SIPS) leads to the build up of stratification during the ebb and a breakdown during the flood. Since the straining component is negative during the flood flow, the stratification cycle observed at the mouth of San Diego Bay could be explained by either advection of the non-zero longitudinal stratification gradient, or on the basis of variations in local vertical mixing rates (Figure 7).

Concluding Remarks

We have examined, from an observational viewpoint, the role of thermal stratification in the tidal exchange process at the mouth of San Diego Bay. We found that the structure of the outflow, and the nature of the tidal exchange process both appear to be influenced by thermal stratification. The tidal outflow is found to lift-off from the bottom during the initial and later stages of the ebb flow when barotropic forcing is weak. During the peak ebb flow, the exit Froude number becomes supercritical, the mouth section is flooded, and the outflow extends to the bottom. As the ebb flow weakens, the Froude number transitions to subcritical, and a period of two-way exchange occurs, with the surface layer flowing seaward, and the deep layer flowing into the bay. The structure of the tidal residual flow and the residual transport of a measured tracer (UVF) are strongly influenced by this vertical exchange. Exchange appears to occur laterally as well in a manner consistent with the tidal pumping mechanism. Tidal cycle variations in shear and stratification are characterized by strong vertical shear and breakdown of stratification during the ebb, and weak vertical shear and build-up of stratification on the flood. Evaluation of multiple tidal cycles from time-series records of flow and temperature indicate that the vertical variations of the flow and stratification observed during the cross-sectional

measurements are a general phenomenon during the summer. Together, these observations suggest that thermal stratification can play an important role in regulating the tidal exchange of low-inflow estuaries.

Acknowledgements

This work was supported by grants from the Naval Command, Control, and Ocean Surveillance Center (#ZW86524A01), the California Regional Water Quality Control Board (IAA #1-188-190-0), and the California Department of Boating and Waterways (IAA #93-100-026-13). Field work and data processing was made possible by support from Chuck Katz, Andy Patterson, Brad Davidson, Kimball Millikan, Ron George, and Jeff Gartner.

List of Figures

Figure 4. Cross-sectional contours of (a) axial velocity, (b) temperature, and (c) UVF from the tidal cycle transects of May 17, 1994. Transect times are shown on each plot. Velocity sections were interpolated from shipboard ADCP measurements at 1 meter vertical spacing between about 2 meters below the surface and 2 meters above the bottom. Positive velocities flow into the bay. Temperature and UVF sections were interpolated from a series of 7 vertical "tow-yo" casts (14 profiles), an example is shown the first plate of the temperature sections. From the velocity sections, note the strong vertical velocity shear during the ebb flow, the period of exchange flow during low-water, and the absence of vertical shear during the flood.

Figure 5. Axial temperature sections through the mouth of San Diego Bay. Sections are interpolated from vertical CTD profiles obtained at 1 kilometer spacing (see triangles) on May 17, 1994. Transect times are shown on each plot. The bold arrows indicate the relative magnitude and direction of the barotropic tidal current. Note the thermal wedge present at high-water, its breakdown at the mouth during the ebb, and its reestablishment during the subsequent flood.

Figure 6. Axial velocity sections through the mouth of San Diego Bay. Sections are based on shipboard ADCP measurements obtained during the mapping surveys on May 18, 1994. Transect times are shown on each plot, and the numbers in parentheses indicate the corresponding temperature transect from Figure 5 based on similar tide stage. Strong vertical shear and liftoff of the outflow are observed during the early stage ebb. During the period of strong ebb, the flow remains bottom-attached, but appears to liftoff again as the ebb weakens prior to flood. Note the vertical exchange during the transition from ebb to flood, and the strong

flow at depth during the early stages of the flood.

Figure 7. Tidal cycle evolution of (a) surface and bottom layer velocity and velocity at various depths, (b) layer Froude (F_i^2) number and normalized interface height, (c) surface-bottom stratification, and (d) Richardson number. All values were developed from laterally averaged profiles from the channel region of the mouth transects (cross channel distance 750-1250 m). Surface and bottom layer velocities are averaged values above and below the zero-velocity interface. Layer Froude numbers are caluclated from the averaged layer velocities and densities. The Richardson number is the minimum value for a given profile. Strong vertical shear is present during the ebb and a period of exchange flow occurs during the ebb-flood reversal, corresponding to transitions from critical to sub-critical Froude number. Note the development of stratification during the late flood and the correspondingly high Richardson numbers.

Figure 8. Tidally-averaged residuals from the cross sectional transects of May 17, 1994 for (a) velocity (positive into the bay), (b) UVF concentration, and (c) UVF transport (positive into the bay). The residual velocity is outward at the surface and inward at depth and on the western side of the channel. High UVF is concentrated in the surface, leading to a net vertical exchange with strong outward transport at the surface, and a weaker return of material primarily through the deep part of the channel where the intrusion of the thermal wedge is most pronounced.

Figure 9. Temperature-UVF mixing diagram based on the cross sectional measurements at the mouth on May 18, 1994. Curves are shown for the complete cross-sectional average, surface section ($z < 6$ m) average, and bottom section average ($z > 6$ m). During the ebb, the section

transitions from cold, low-UVF oceanic water to warm, high-UVF bay water. On the flood, lateral exchange (tidal pumping) is evident as warm, low-UVF surface ocean water first enters the section, followed by a period of vertical exchange as the cold, low UVF thermal wedge intrudes.

Figure 10. Time-series evolution of surface and bottom velocity from the bottom mounted ADCP during the period June 3 - June 18, 1993. Strong vertical shear is apparent during all ebb tides. The bottom velocity tends to lead the surface velocity during the ebb-flood reversal, especially during periods of neap tides (see Julian day 190-192). Vertical shear during the neaps is comparable to or greater than during the springs, suggesting enhanced baroclinic circulation during periods of weak tidal mixing.

Figure 11. Time-series variations in thermal stratification from the thermistor string at the mouth during the period July 29 - 2 August, 1993. Tides are similar to those shown for days 185-190 in the ADCP record in Figure 10. On the strong ebb flows, the thermal stratification breaks down entirely, followed by a rapid rebuilding during the ebb-flood transition. On the weak ebb flows, the stratification may break down partially or remain unaffected.

References

Armi, L. and D. Farmer, 1986. Maximal two-layer exchange through a contraction with barotropic net flow. *J. Fluid Mech.*, **164**:27-51.

Dyer, K.R., 1974. The salt balance in stratified estuaries. *Estuarine Coastal Marine Science*, **2**:275-281.

Gartner, J.W., R.T. Cheng, and K.R. Richter, 1994. Hydrodynamic characteristics of San Diego Bay, California - Part II, recent hydrodynamic data collection. *EOS, Transactions, American Geophysical Union*, **75**(3):60.

Hammond, R.R., 1976. Seabed drifter movement in San Diego Bay and adjacent waters. Naval Undersea Research and Development Center, San Diego, CA, Technical Report No. TP507.

Katz, C.N. and D.B. Chadwick, 1991. Real-time fluorescence measurements intercalibrated with GC-MS. *Proceedings, Oceans 1991*, **1**:351-358.

Katz, C.N., L. Skinner, and D.B. Chadwick, (in prep.). In-situ leach rate measurements from creosote impegnated pier pilings.

Largier, J.L., C.J. Hearn, and D.B. Chadwick, 1995a. Density structures in low-inflow, seasonal

estuaries. Submitted to: *Proceedings of the 7th International Biennial Conference on Physics of Estuaries and Coastal Seas, November, 1994, Woods Hole, MA.*

Largier, J.L., J.T. Hollibaugh, and S.V. SMith, 1995b. Seasonally hypersaline estuaries in mediterannean climatic regions. Submitted to: *Estuarine, Coastal and Shelf Science.*

Nunes Vaz, R.A. and J.H.Simpson, 1994. Turbulence closure modeling of estuarine stratification. *J. Geophys. Res.*, 99(C8):16143-16160.

Peeling, T., 1974. A proximate biological survey of San Diego Bay, California. Naval Undersea Research and Development Center, San Diego, CA, Technical Report No. TP389.

Signell, R.P. and B. Butman,1992. Modeling tidal exchange and dispersion in Boston Harbor. *J. Geophys. Res.*, 97(C10):15591-15606.

Simpson, J.H., J. Sharples, and T.P. Rippeth, 1991. A prescriptive model of stratification induced by freshwater run-off, *Estuarine Coastal Shelf Sci.*, 33:23-35.

Smith, E.L., 1972. Temperature fluctuations at a fixed position in San Diego Bay. Naval Undersea Research and Development Center, San Diego, CA, Technical Report No. TP298.

Stommel, H. and H.G. Farmer, 1952. On the nature of estuarine circulation. Part II, Woods Hole Oceanogr. Inst. Tech. Rep. WHOI-52-51, Woods Hole, Mass.

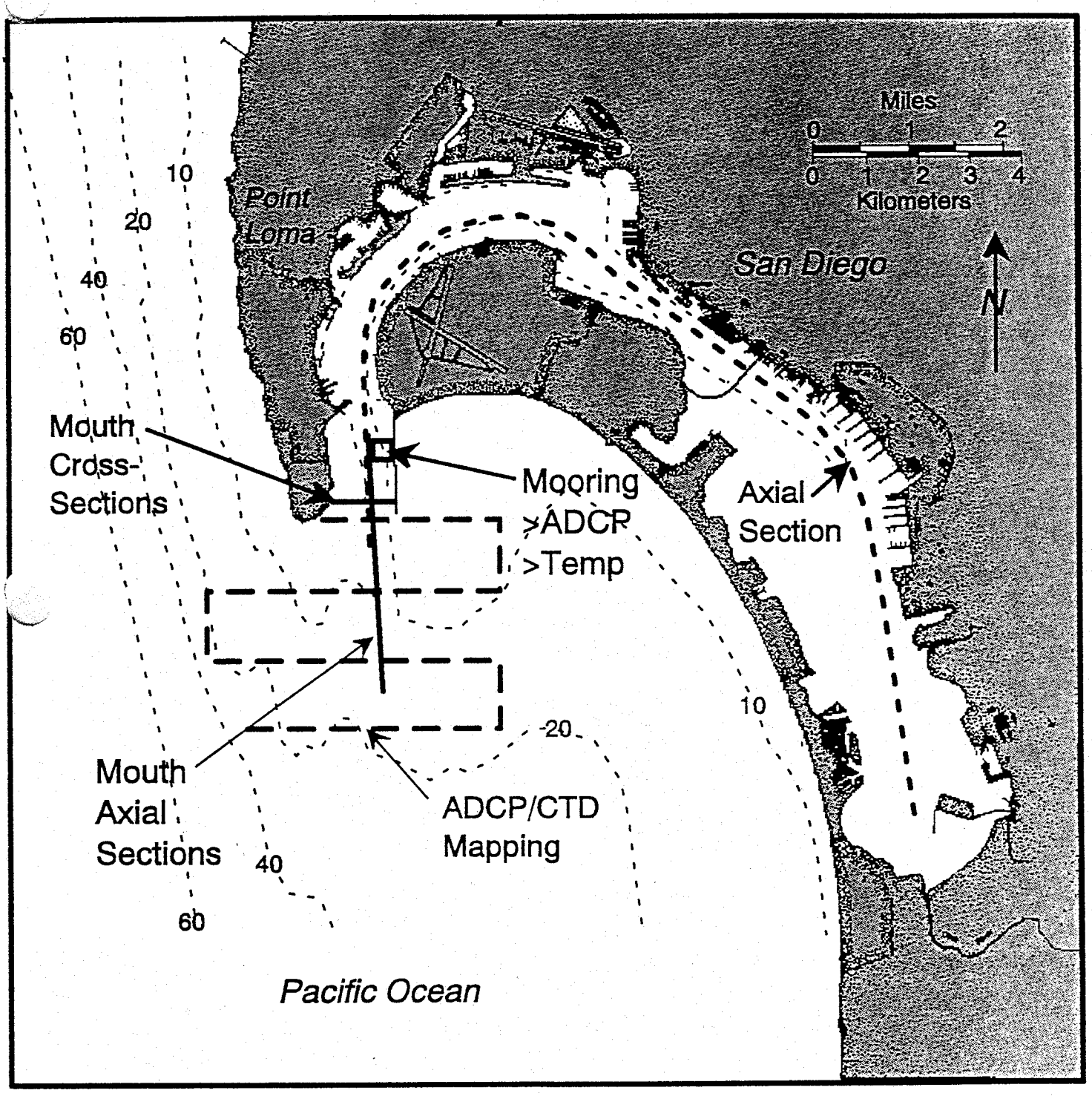
Miles
0 1 2
0 1 2 3 4
Kilometers
N
Point Loma
San Diego
10
20
40
60
Mouth Cross-Sections
Mooring >ADCP >Temp
Axial Section
Mouth Axial Sections
ADCP/CTD Mapping
10
20
40
60
Pacific Ocean

FIGURE 1

a) **Summer**

b) **Winter**

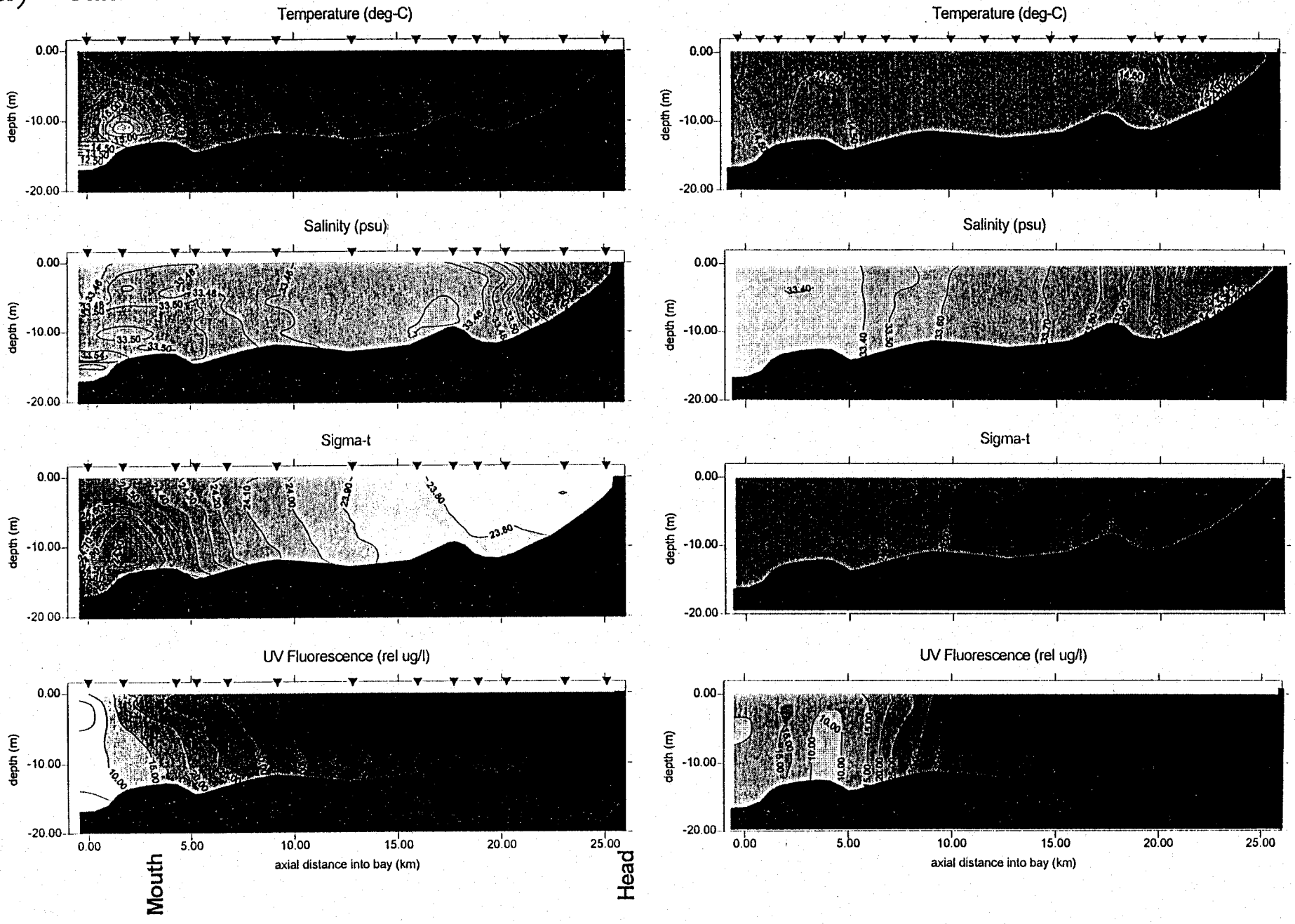

FIGURE 2

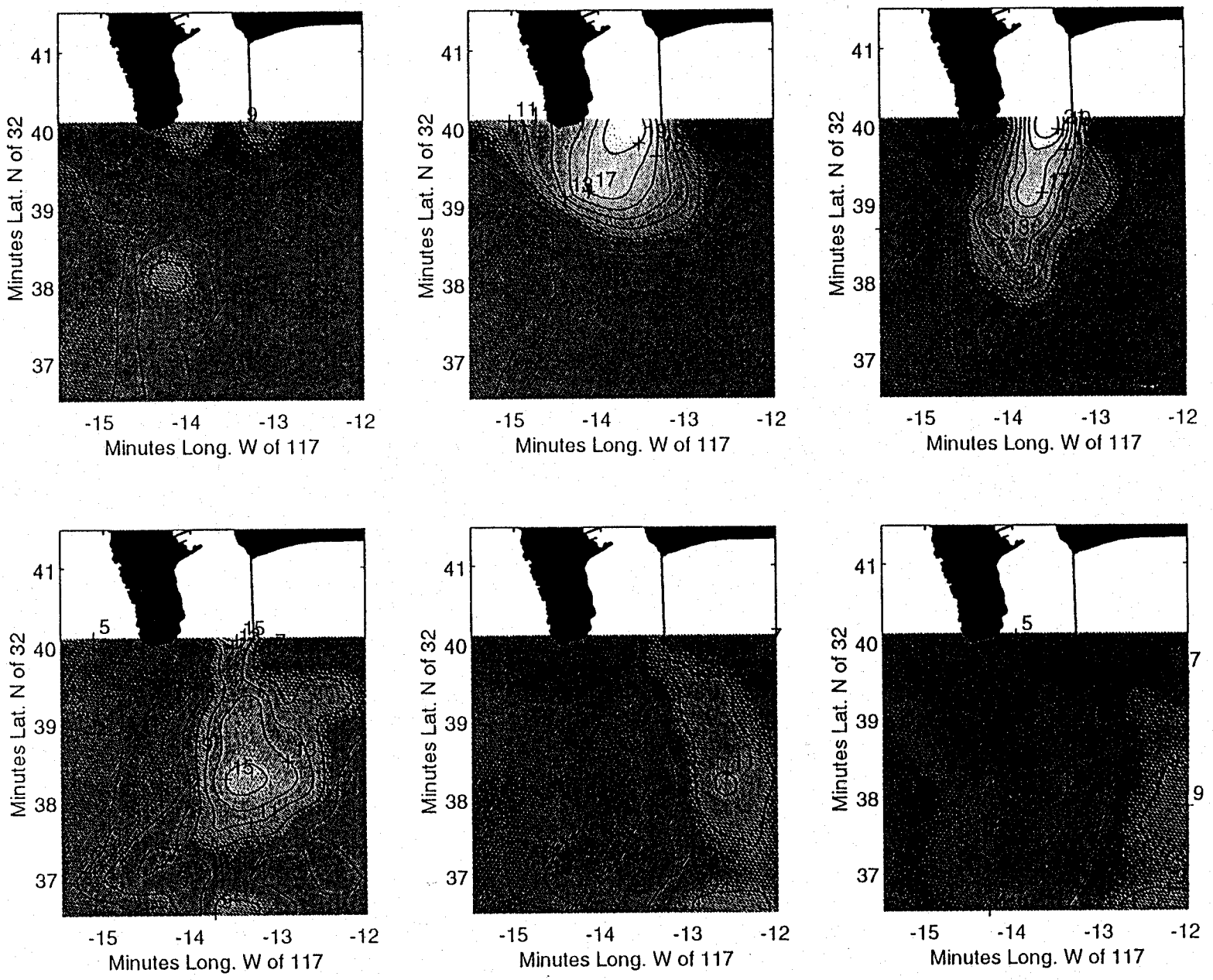
41
40
39
38
37
Minutes Lat. N of 32
-15
-14
-13
-12
Minutes Long. W of 117

FIGURE 3

a) North Velocity (into bay = + cm/s)

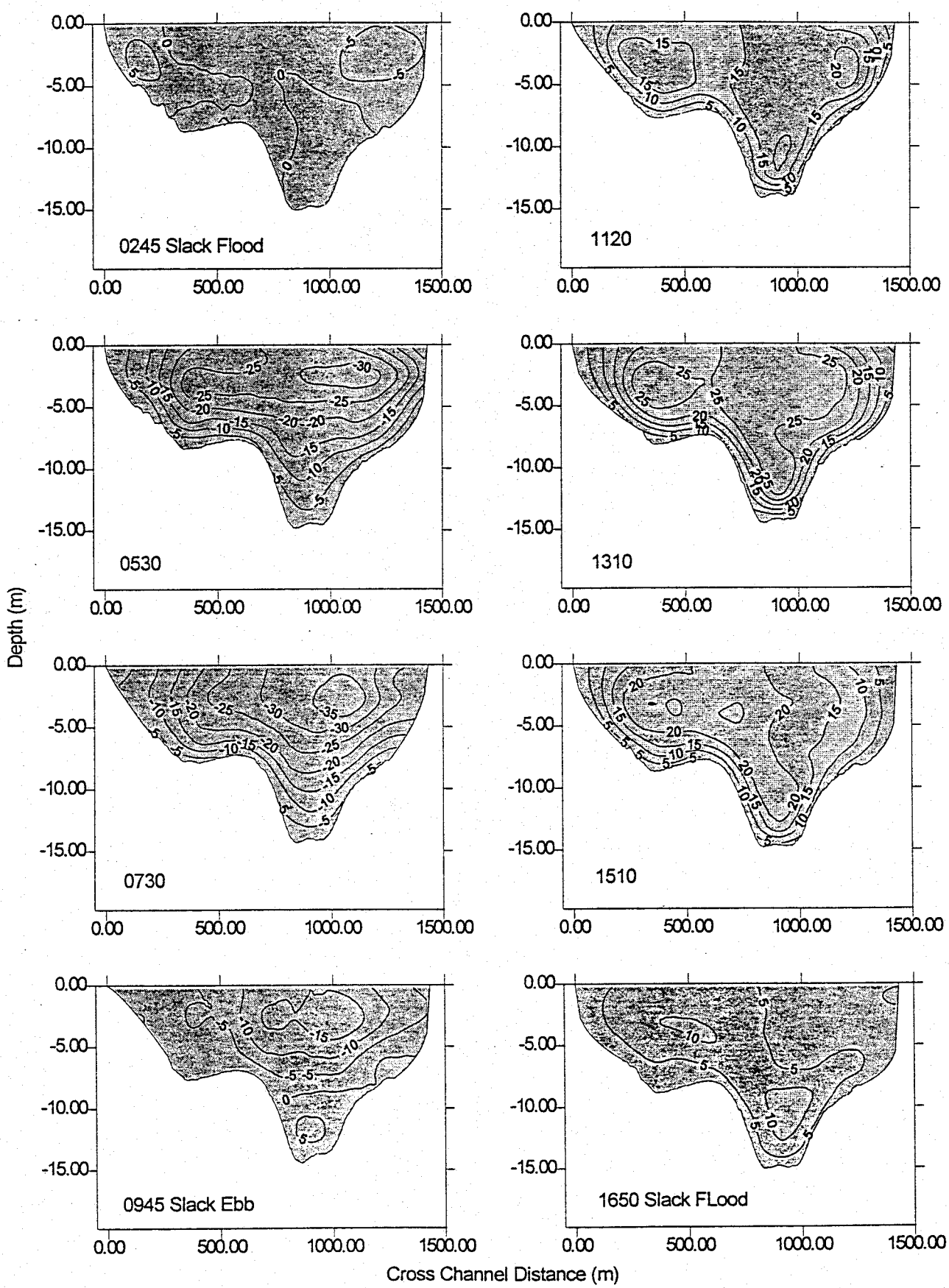

FIGURE 4

b) Temperature (deg C)

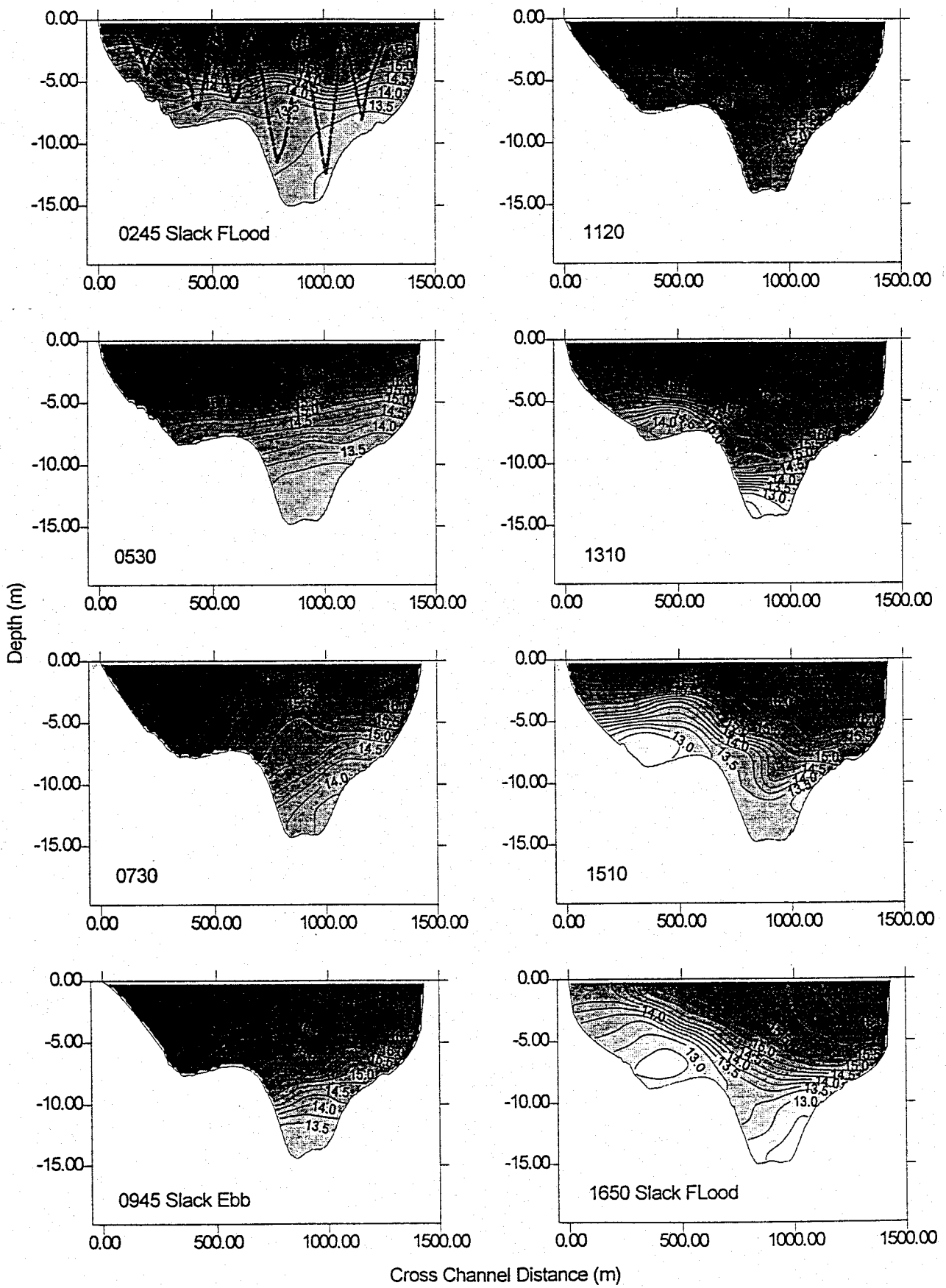

FIGURE 4

c) UV Fluorescence (rel ug/l)

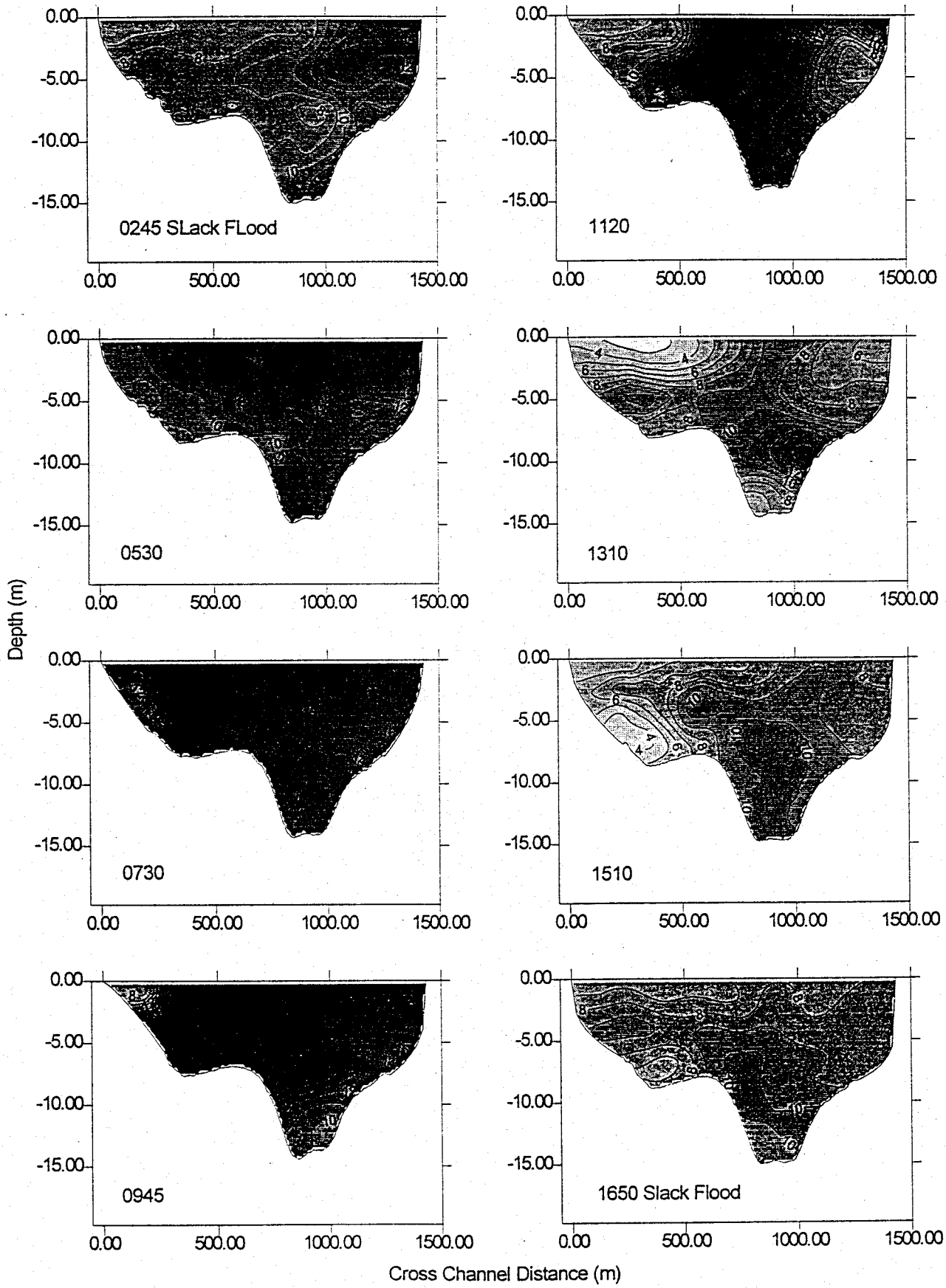

FIGURE 4

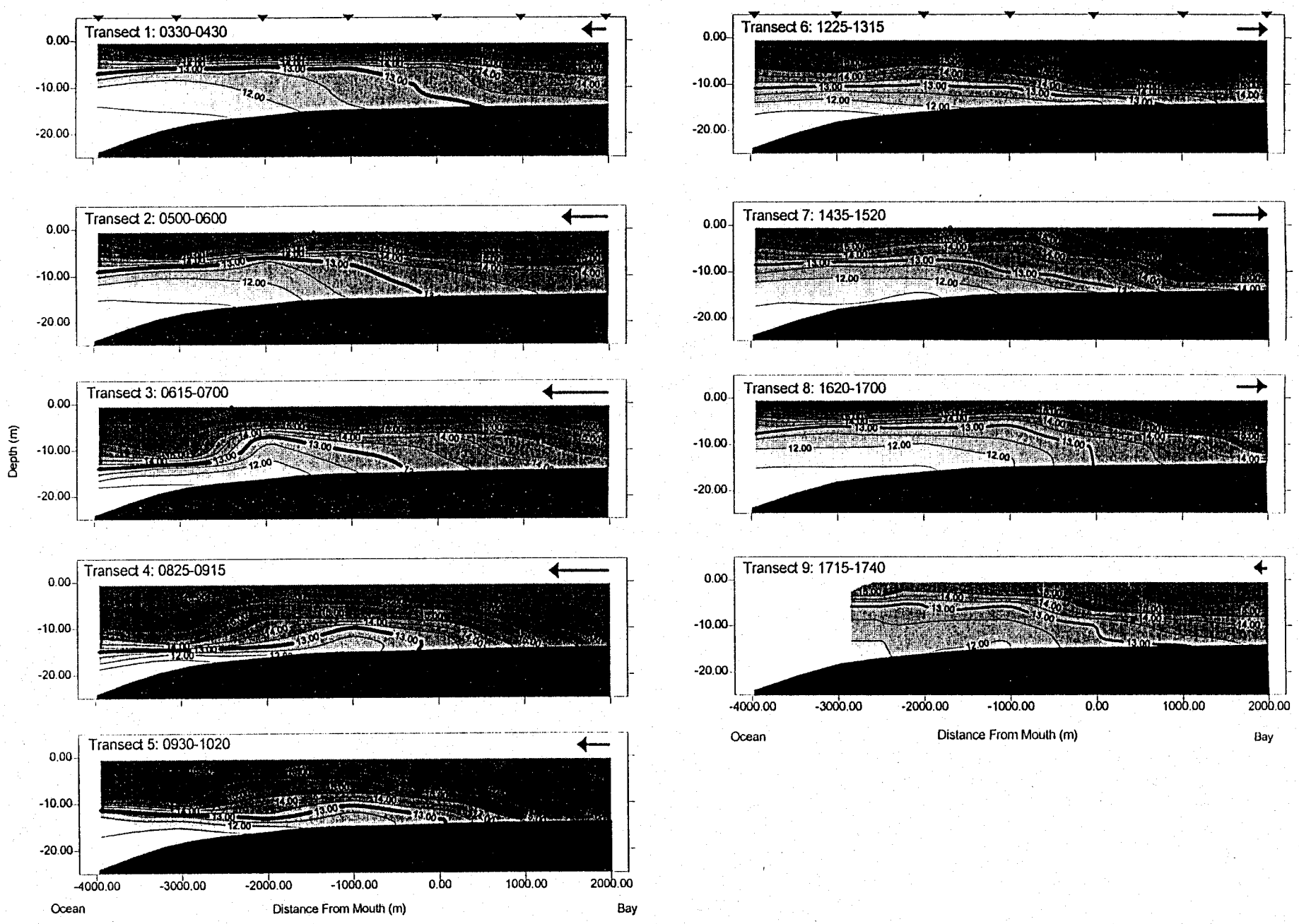
Transect 1: 0330-0430
Transect 2: 0500-0600
Transect 3: 0615-0700
Transect 4: 0825-0915
Transect 5: 0930-1020
Transect 6: 1225-1315
Transect 7: 1435-1520
Transect 8: 1620-1700
Transect 9: 1715-1740
Depth (m)
0.00
-10.00
-20.00
-4000.00
-3000.00
-2000.00
-1000.00
0.00
1000.00
2000.00
Ocean
Distance From Mouth (m)
Bay

FIGURE 5

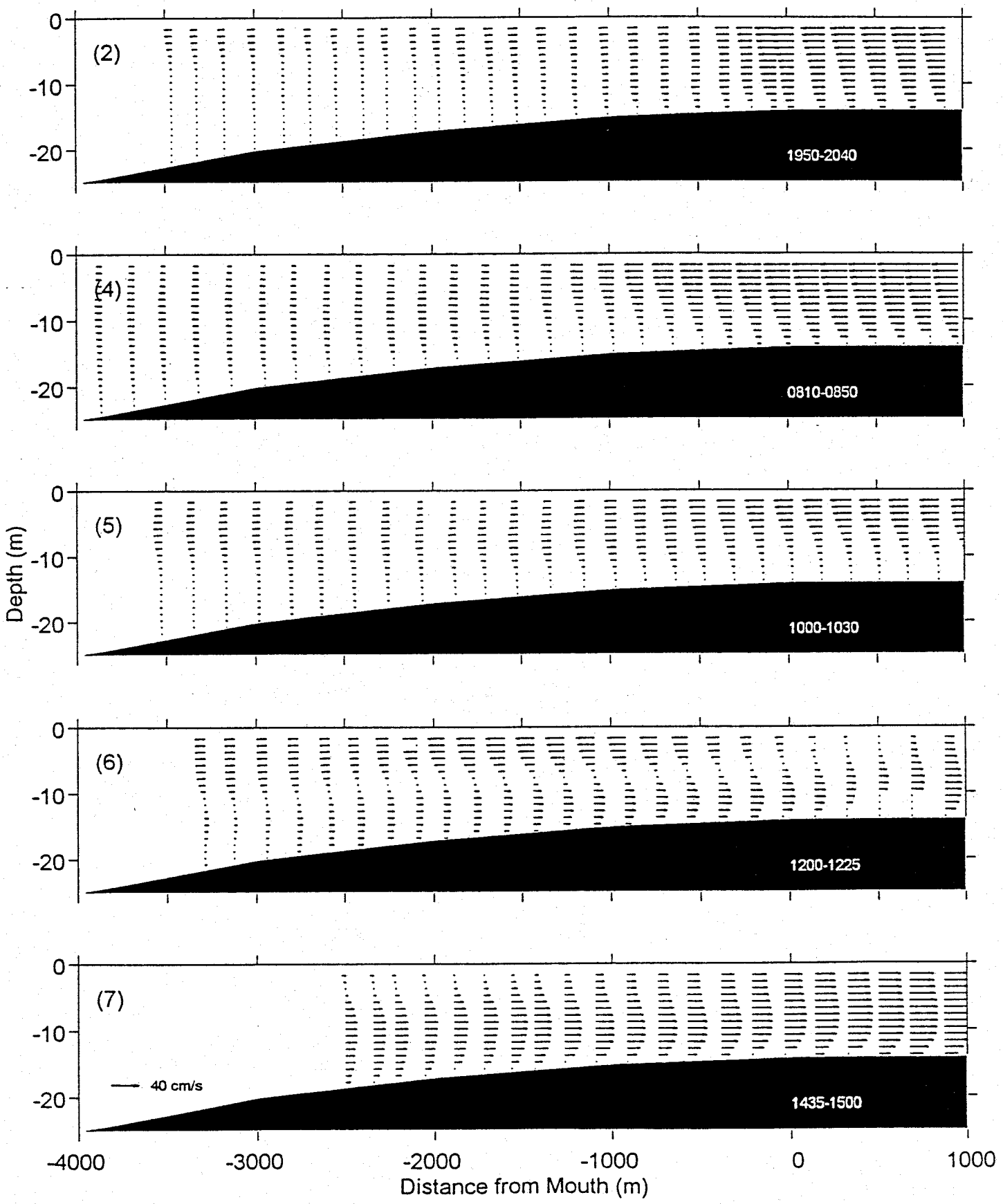
(2)
1950-2040
(4)
0810-0850
(5)
1000-1030
(6)
1200-1225
(7)
1435-1500
40 cm/s
0
-10
-20
Depth (m)
-4000
-3000
-2000
-1000
0
1000
Distance from Mouth (m)

FIGURE 6

a)

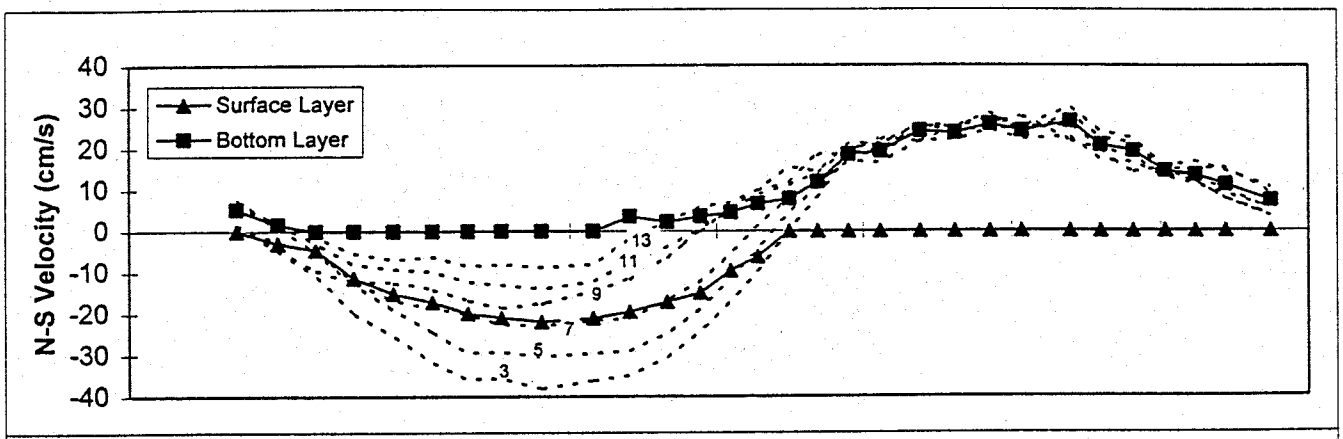

b)

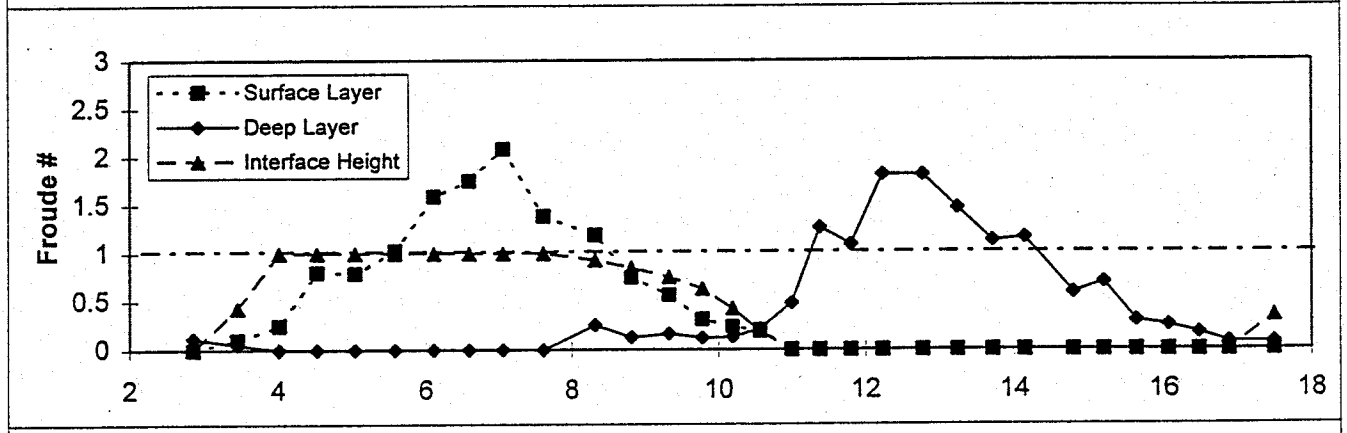

c)

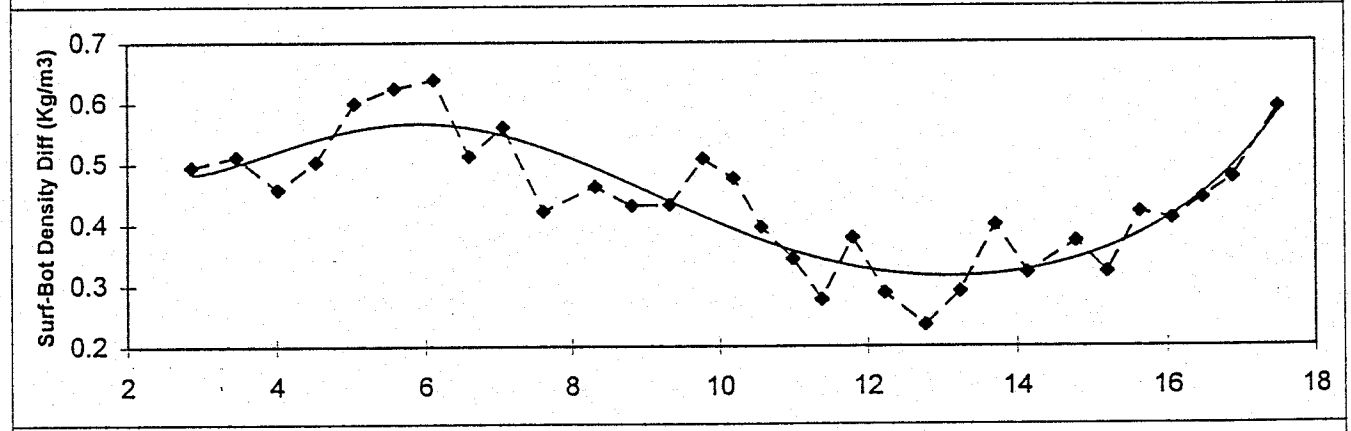

d)

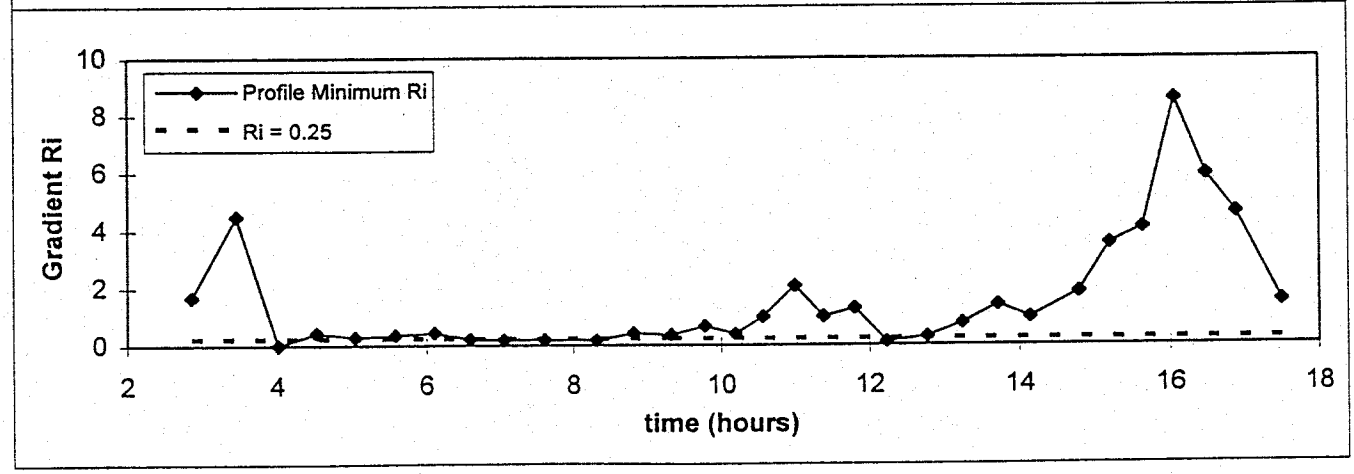

FIGURE 7

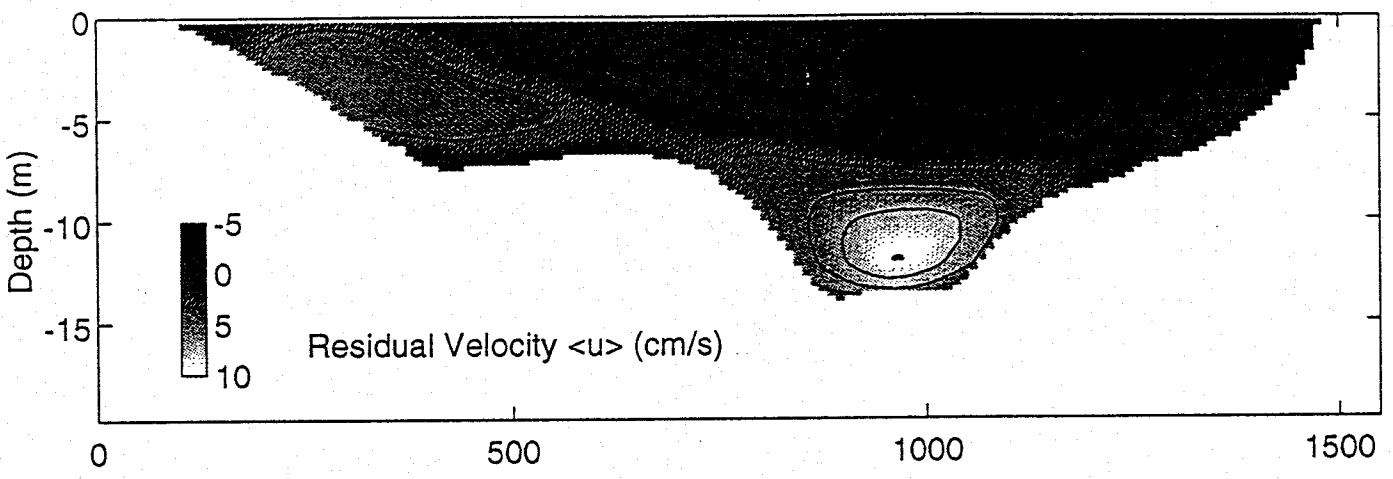
0
-5
-10
-15
Depth (m)
-5
0
5
10
Residual Velocity <u> (cm/s)
0
500
1000
1500

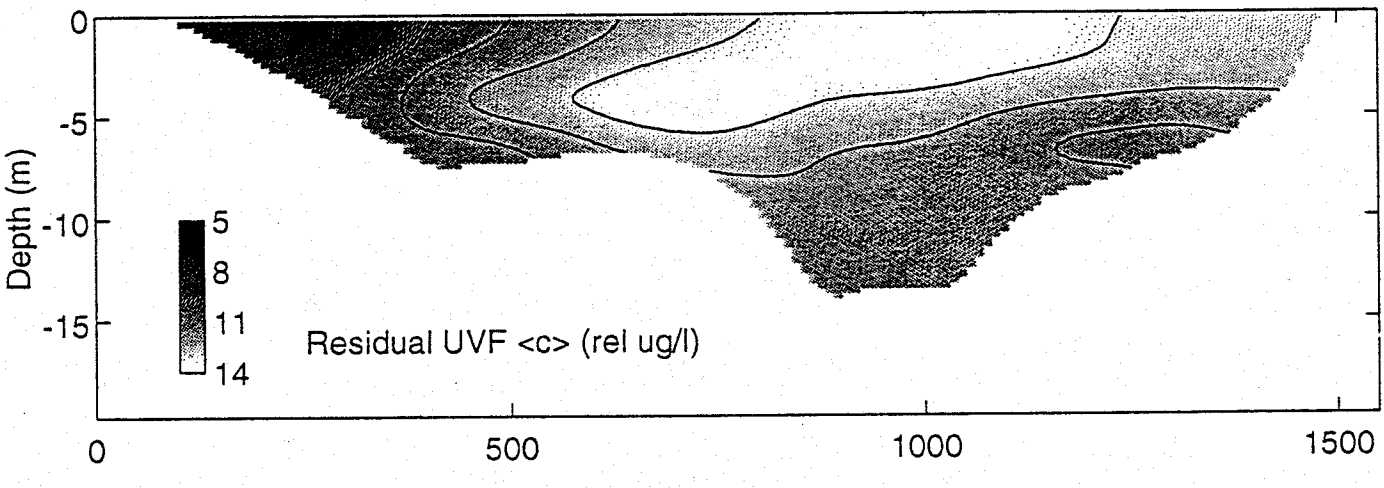
0
-5
-10
-15
Depth (m)
5
8
11
14
Residual UVF <c> (rel ug/l)
0
500
1000
1500

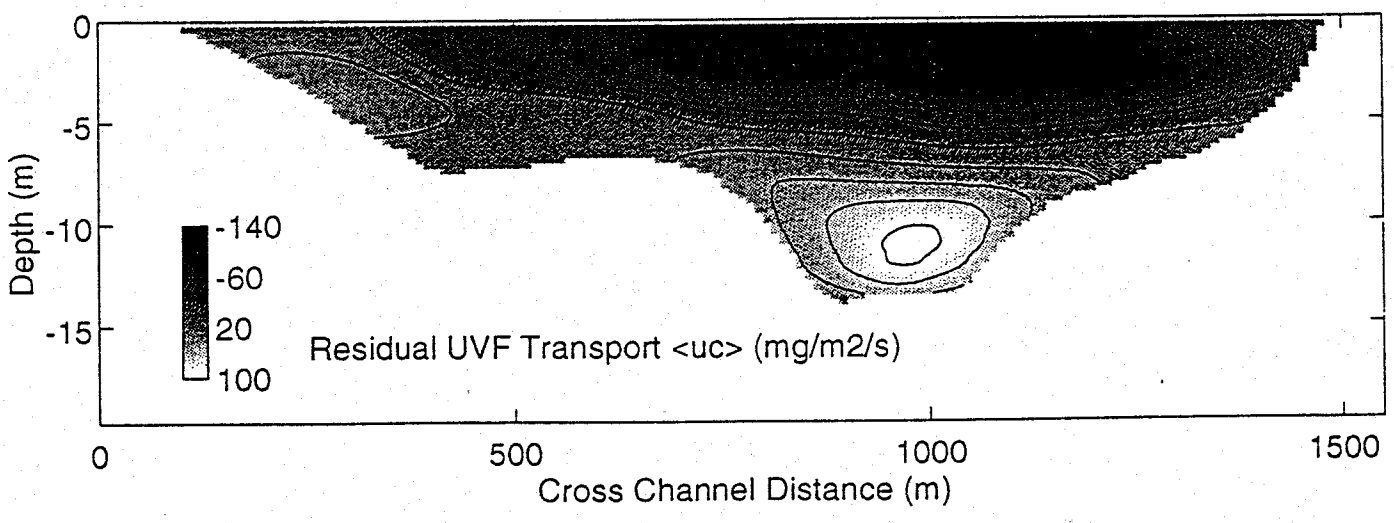
0
-5
-10
-15
Depth (m)
-140
-60
20
100
Residual UVF Transport <uc> (mg/m2/s)
0
500
1000
1500
Cross Channel Distance (m)

FIGURE 8

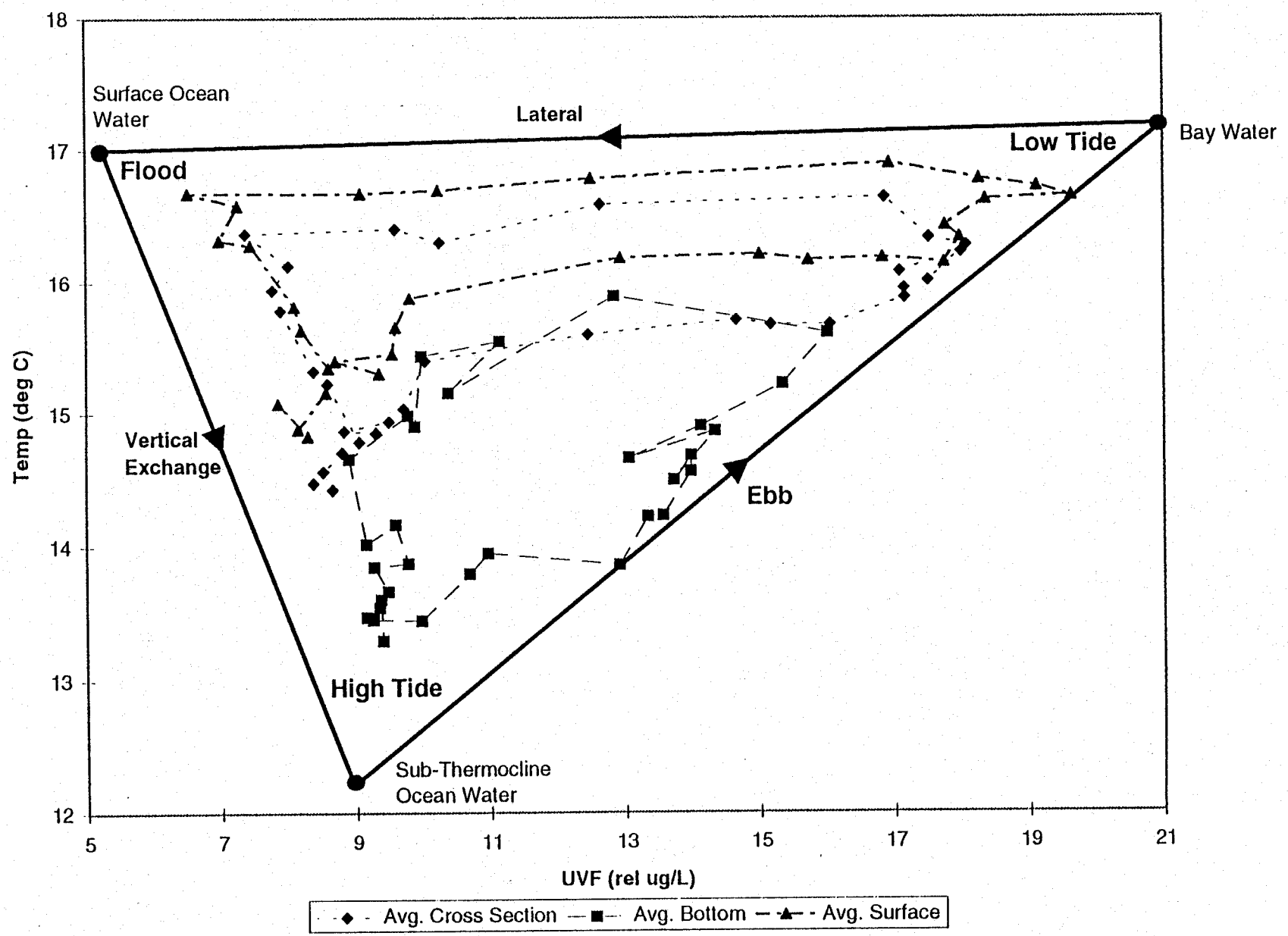
Surface Ocean Water
Lateral
Bay Water
Low Tide
Flood
Vertical Exchange
Ebb
High Tide
Sub-Thermocline Ocean Water
Temp (deg C)
UVF (rel ug/L)
18
17
16
15
14
13
12
5
7
9
11
13
15
17
19
21
Avg. Cross Section
Avg. Bottom
Avg. Surface

Figure 9

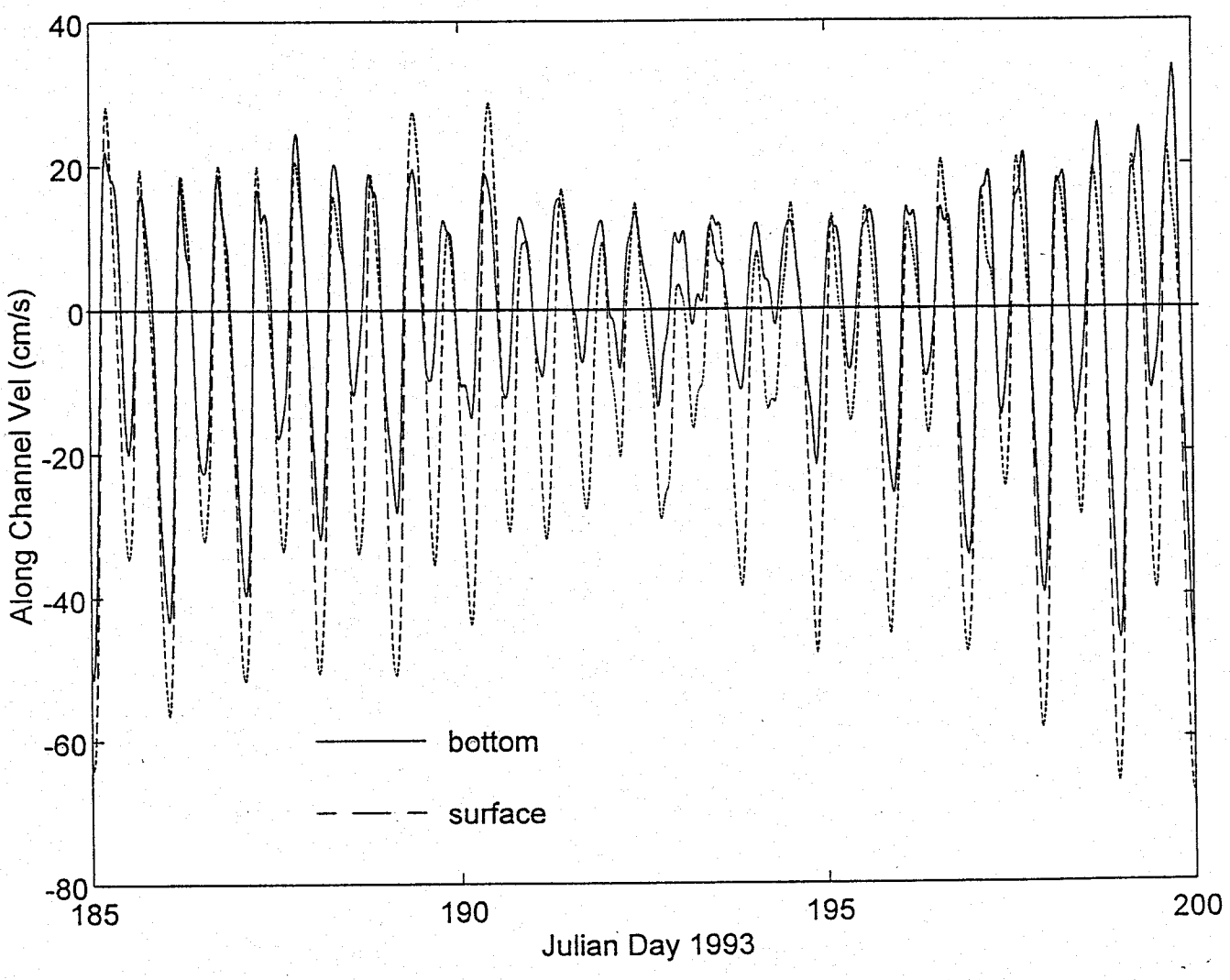
40
20
0
-20
-40
-60
-80
185
190
195
200
Along Channel Vel (cm/s)
Julian Day 1993
bottom
surface

FIGURE 10

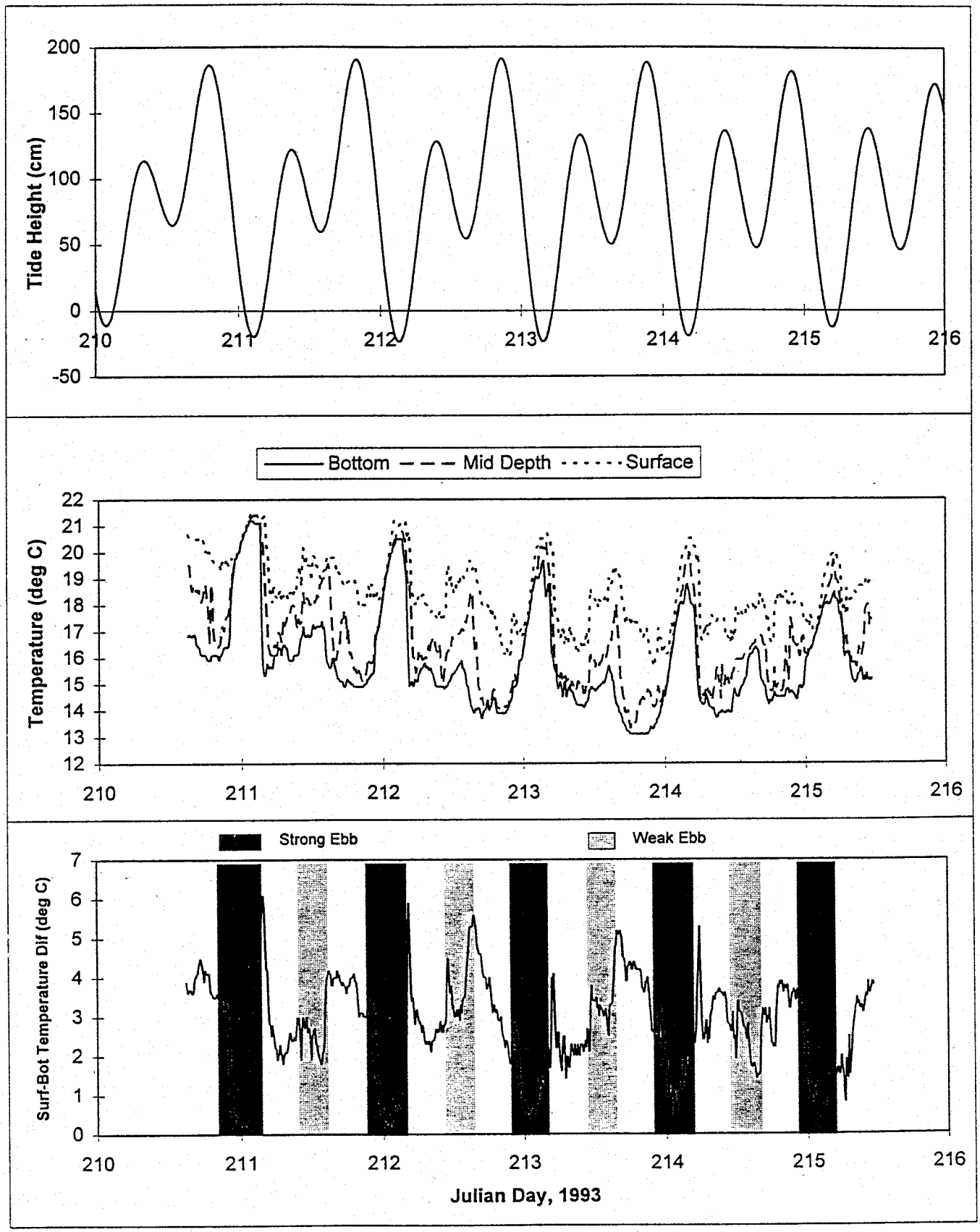
Tide Height (cm)
200
150
100
50
0
-50
210
211
212
213
214
215
216
Bottom
Mid Depth
Surface
Temperature (deg C)
22
21
20
19
18
17
16
15
14
13
12
Strong Ebb
Weak Ebb
Surf-Bot Temperature Dif (deg C)
7
6
5
4
3
2
1
0
Julian Day, 1993

FIGURE 11